JOURNAL OF MAGNETIC RESONANCE **124,** 104–121 (1997)
ARTICLE NO. MN961001

Proton Chemical-Shift Spectra

SVETLANA SIMOVA,* HELMUT SENGSTSCHMID,† AND RAY FREEMAN

Department of Chemistry, Cambridge University, Lensfield Road, Cambridge CB2 1EW, United Kingdom

Received August 29, 1996

Three related methods are explored for obtaining high-resolution proton spectra without spin–spin splittings, termed ''chemical-shift spectra.'' They are based on two-dimensional *J* spectroscopy, where the F_1 dimension is derived by Fourier transformation of spin-echo modulation. The first technique superimposes the *J* spectrum on its reflection in the $F_1 = 0$ axis, creating multiplet patterns in the form of a St. Andrew's cross. The other two techniques purge certain antiphase product-operator terms, either by dispersal in an inhomogeneous effective radiofrequency field oriented at the magic angle (54.7°) or by means of a *z* filter. In all three cases, the two-dimensional multiplets are separated by means of a symmetry filter and their centers are taken as a measure of the respective chemical shifts. The 400 MHz proton chemical-shift spectrum of 4-androsten-3,17-dione is presented as an illustrative example. Good separation is achieved, even for interpenetrating spin multiplets with near degeneracies in their chemical shifts. Complications due to strong-coupling effects are discussed.

INTRODUCTION

It would be a great simplification if high-resolution proton NMR spectra could be recorded in a mode where all spin–spin splittings were eliminated and the resonance frequencies were determined purely by chemical-shift effects. Analysis and assignment would then be more straightforward, and the display of time-dependent spectra, for example, spin–lattice relaxation curves, would be greatly simplified. Ideally, if the spin–spin relaxation times are relatively uniform, such a ''chemical-shift spectrum'' would have integrals that reflected the numbers of equivalent protons at each site, and many spectra would have uniform intensities, apart from the resonances of methyl or equivalent methylene protons. In fact, we might anticipate better uniformity of intensities than that observed in decoupled ^{13}C spectroscopy, where the nuclear Overhauser enhancement introduces an additional variable factor.

The general principles behind such an experiment were first elucidated by Aue *et al.* (*1*). A two-dimensional proton *J* spectrum (*2*), obtained by Fourier transformation of spin echoes, has only spin multiplets in the F_1 dimension, with the conventional coupled proton spectrum in the F_2 dimension. Consequently the spin multiplets are aligned along 45° diagonals of the two-dimensional spectrum and a 45° projection should give singlet responses at the chemical-shift frequencies with no spin–spin splittings. In practice there are serious complicating factors arising from the curious ''phase-twist'' lineshape (*3*) observed in this kind of spectrum, and the 45° projection of a phase-sensitive *J* spectrum simply vanishes (*4*). Despite the considerable effort expended on this problem (*5–12*), a generally applicable solution has proved elusive. The cases of real interest are those where the conventional high-resolution spectrum contains severely overlapping spin multiplets. There are also serious complications occasioned by strong-coupling effects.

THREE TYPES OF *J* SPECTRA

We consider three related approaches to this problem. Each of these produces a two-dimensional *J* spectrum in a form where the individual multiplets have C_{4v} symmetry. This property is exploited in a search program that locates the symmetry centers even in cases of severe overlap, generating a proton chemical-shift spectrum. The three methods involve different degrees of complication in the experimental methodology, and different degrees of success in handling crowded proton spectra. They all produce acceptable results for severely congested regions of a test case—the 400 MHz proton spectrum of 4-androsten-3,17-dione—in spite of complications due to strong-coupling effects.

Reflected J Spectra

This method (*12*) employs the unmodified spin-echo technique

$$90°—\tfrac{1}{2}t_1—180°—\tfrac{1}{2}t_1—\text{acquire}. \qquad [1]$$

In the normal mode of data processing this would generate spin multiplets lying along 45° diagonals, with the individual

* On leave from the Institute of Organic Chemistry, Bulgarian Academy of Sciences, Sofia, Bulgaria.

† On leave from the Institut für Organische Chemie, Karl-Franzens Universität, Graz, Austria.

1090-7807/97 $25.00

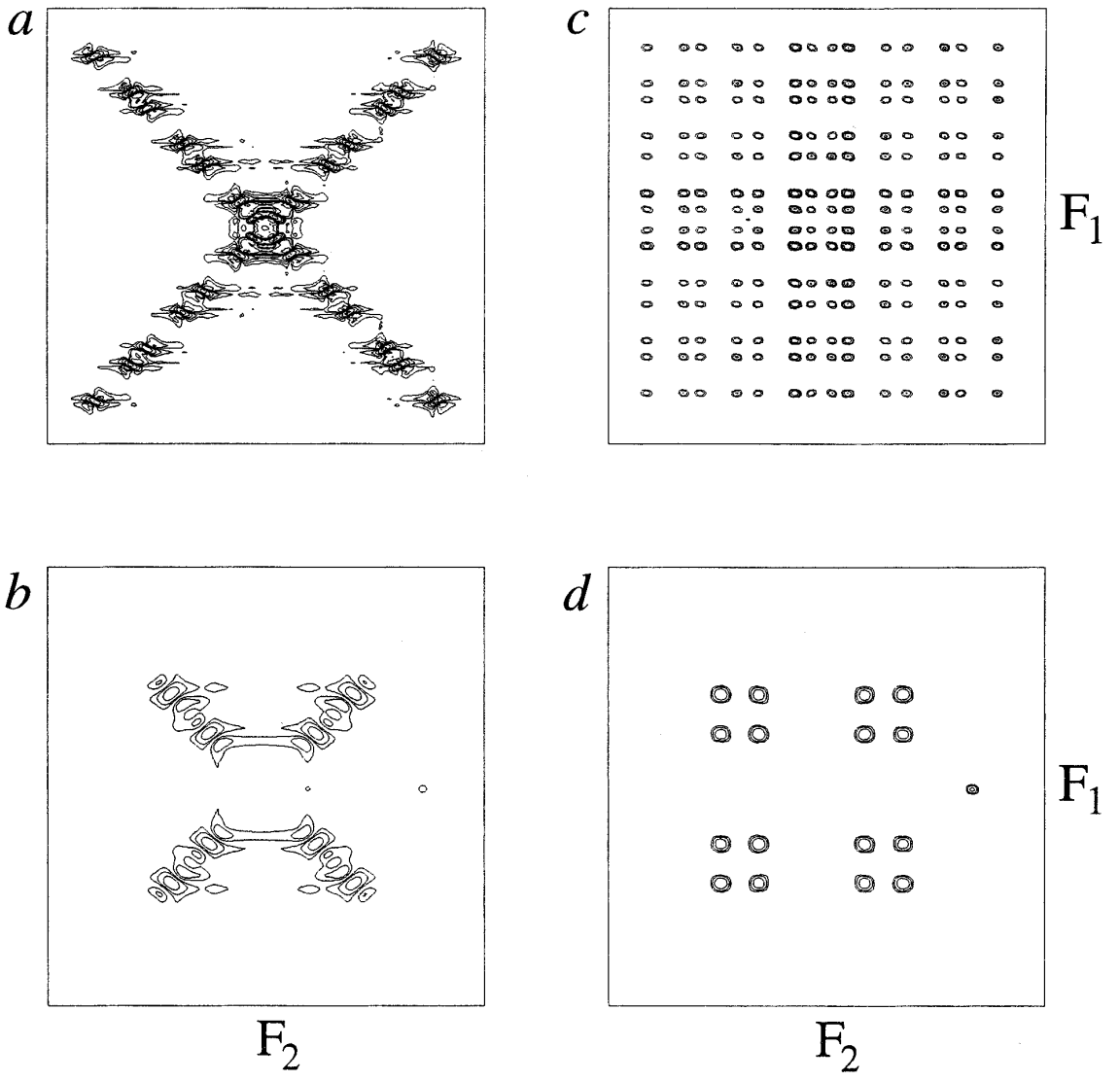

FIG. 1. Typical spin multiplets (40 by 40 Hz) from the unprocessed 400 MHz proton *J* spectrum of borneol. Multiplet (a) at 2.28 ppm and multiplet (b) at 0.95 ppm are from the reflected *J* spectrum and have individual resonances with the phase-twist lineshape, lying on the 45° or 135° diagonals. The corresponding multiplets (c) and (d) are from the *z*-filtered *J* spectrum and are in pure absorption, having a structure generated by multiplication of the one-dimensional multiplet in the F_1 dimension by an identical pattern in the F_2 dimension. Note that these spectra are better resolved in the F_1 dimension than in F_2 because of the refocusing effect.

resonances in the form of a phase-twist lineshape (the superposition of a two-dimensional absorption signal on a two-dimensional dispersion signal of the same intensity). However, if a real Fourier transform (instead of the usual complex Fourier transform) is performed in the t_1 dimension, there is no sign discrimination in the F_1 dimension, and the *J* spectrum is superimposed on its reflection in the $F_1 = 0$ axis. The multiplets then form a St. Andrew's cross, still retaining the phase-twist shape, except for resonances at the F_1 frequency origin where the dispersion-mode components cancel. Typical patterns taken from the spectrum of borneol (2-*endo*-bornyl alcohol) are illustrated in Figs. 1a and 1b. Projections onto the F_1 or F_2 axes give spin multiplets in the pure absorption mode because the dispersion-mode contributions cancel identically.

The main advantage of this method is that it is simple to implement, requiring no modification of the basic spin-echo pulse sequence. In principle, the St. Andrew's-cross pattern should involve less overlap of adjacent multiplets than the other two methods, but in practice the phase-twist lineshape complicates the effects of overlap and this constitutes a serious disadvantage. As a result, discrimination between adjacent multiplets may be incomplete and the resulting chemical-shift spectrum exhibits nonuniform intensities.

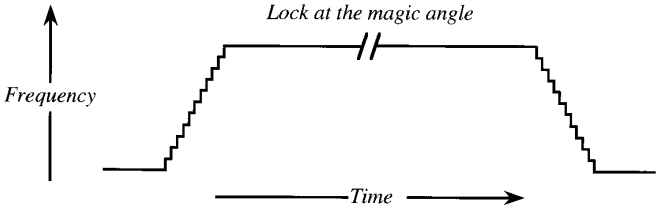

FIG. 2. The adiabatic frequency-sweep function used to take the effective radiofrequency field from the x axis to the magic angle (54.7°) with respect to the z axis, to hold it at this orientation for a time of the order of 25 ms, and then to return it to the x axis. The two adiabatic ramps consist of 11 steps of 300 Hz, each of 100 μs duration.

Purged J Spectra

This second approach (*10*) involves a modification of the basic spin-echo pulse sequence to purge unwanted antiphase dispersion components corresponding to product-operator terms of the form $2I_xS_z$. After a real Fourier transform, the resulting spectrum is a set of two-dimensional spin multiplets, each forming a symmetrical pattern generated by multiplication of a one-dimensional multiplet in the F_1 dimension by the same multiplet in the F_2 dimension. A typical example is illustrated in Fig. 1d for a doublet of doublets from the 400 MHz spectrum of borneol and for a more complex multiplet from the same spectrum (Fig. 1c). This symmetry property is the key to discriminating each two-dimensional multiplet from overlapping neighbors.

The pulse sequence for purged J spectroscopy may be written

$$90^\circ_{\phi_1}\text{—}\tfrac{1}{2}t_1\text{—}180^\circ_{\phi_2}\text{—}\tfrac{1}{2}t_1\text{—purge}_{\phi_3}\text{—acquire}_{\phi_4}$$

$$\begin{array}{cccc} \phi_1 & 0 & 0 \\ \phi_2 & 1 & 1 \\ \phi_3 & 1 & 3 \\ \phi_4 & 2 & 0 \end{array} \qquad [2]$$

A composite $90^\circ_x 180^\circ_y 90^\circ_x$ pulse may be employed in the

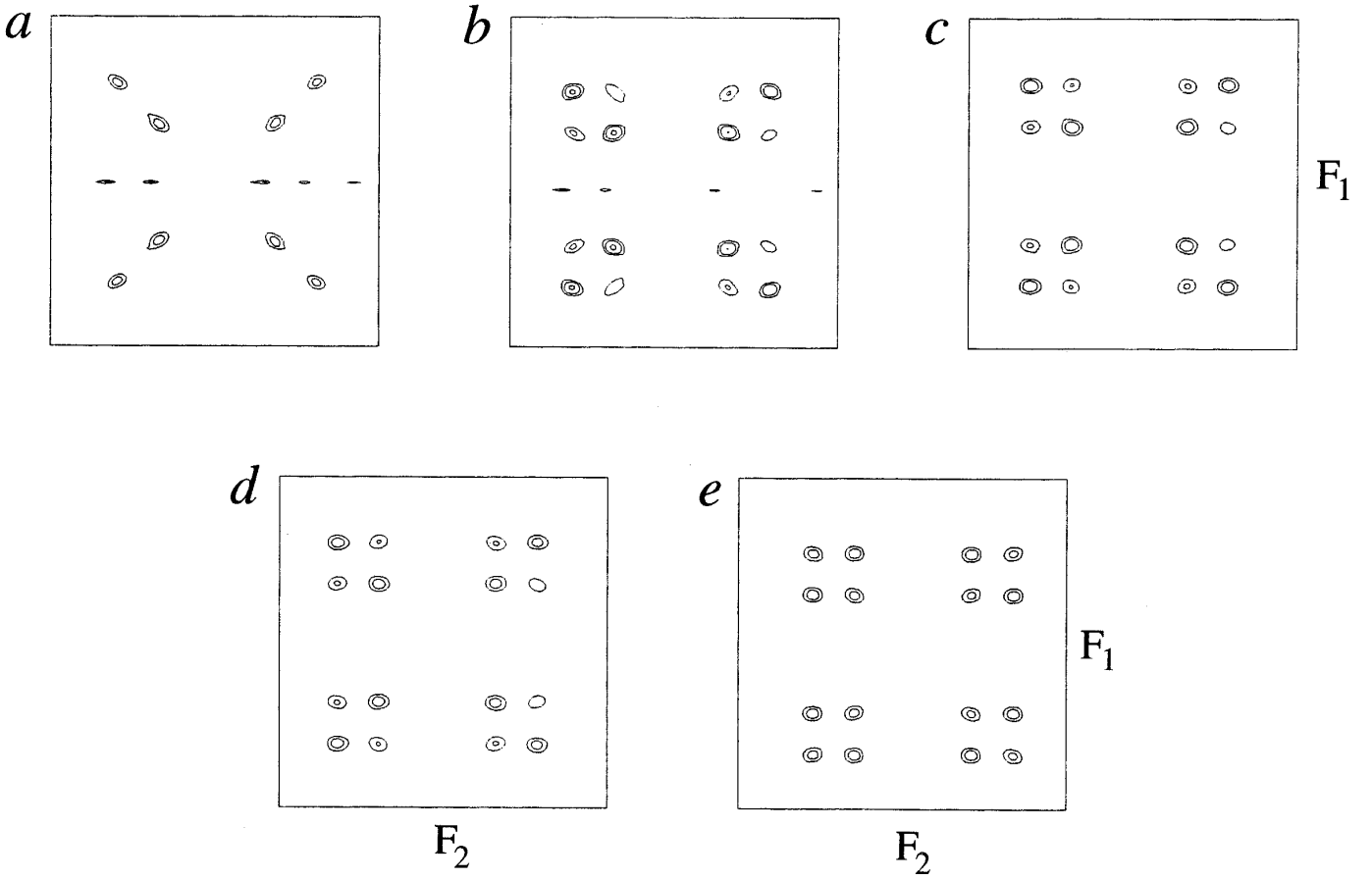

FIG. 3. A typical spin multiplet (26 by 26 Hz) from the 400 MHz two-dimensional proton J spectrum of 4-androsten-3,17-dione, processed by means of a z filter with (a) τ = 20 ms; (b) τ = 20, 4 ms; (c) τ = 20, 4, 15, 10 ms; (d) τ = 20, 4, 15, 10, 12, 30, 7, 27 ms; (e) τ = 20, 4, 15, 10, 12, 30, 7, 27, 1, 33, 16, 8, 21, 36, 40, 29, 21, 14, 38, 5, 35, 2, 31, 25, 11, 23, 3, 24, 15, 9, 19, 13 ms. The progressive cancellation of undesirable product-operator terms leads to increasing intensity for the ''off-diagonal'' resonances.

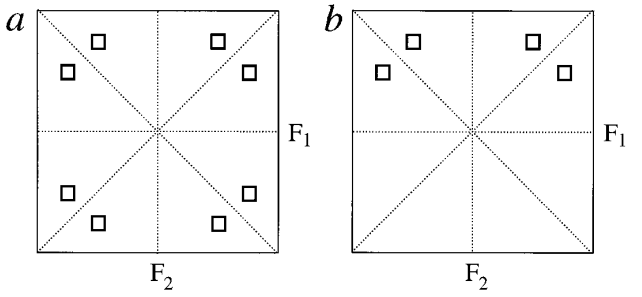

FIG. 4. (a) Within the square test zone, the intensities at eight symmetrically related locations should ideally be the same, and the symmetrization routine replaces them all by the lowest intensity. (b) However, since the intensities at negative F_1 values are identical with the corresponding intensities at positive F_1 values, only four locations need to be tested.

place of the simple 180° pulse. Purging is achieved by dispersing the undesirable components by the spatial inhomogeneity of the effective radiofrequency field B_{eff}, while B_{eff} is oriented at the magic angle (54.7°) with respect to the direction of the applied magnetic field (*13*). This manipulation involves realignment of x magnetization, locking at the magic angle, and subsequent return to the x axis. Figure 2 illustrates the three steps involved: (a) an adiabatic frequency ramp with a typical duration of 1.1 ms, consisting of 11 steps of 300 Hz, starting at resonance and continuing to a point 3300 Hz off-resonance, designed to take the effective field from the x axis to an orientation close to the magic angle; (b) a period of between 25 and 50 ms at constant frequency, locking the magnetization at the magic angle so that the undesirable coherences dephase in the spatial inhomogeneity of the effective field; (c) a second adiabatic ramp of the same duration but in the opposite sense, taking the effective field back to the x axis. Typically the radiofrequency field has an intensity $\gamma B_1/2\pi \approx 4700$ Hz.

It was found that if the period of locking at the magic angle was less than about 10 ms, the suppression of zero-quantum coherence was incomplete and some of the ''off-diagonal'' components of the two-dimensional multiplets were weak or missing; in the limit, the pattern reverted to the general form of the reflected J spectrum (Figs. 1a and 1b). With spin-locking times appreciably longer than 10 ms, some antiphase dispersion components were introduced in the F_2 dimension, leading to baseline distortions.

The great advantage of this method is that, when correctly set up, it gives resonances in pure absorption, thus avoiding the undesirable overlap effects associated with the tails of dispersion-mode signals. The spin-multiplet structure from each individual site can be obtained by projection of the symmetrized spin multiplet onto the F_1 or F_2 axis. Compared

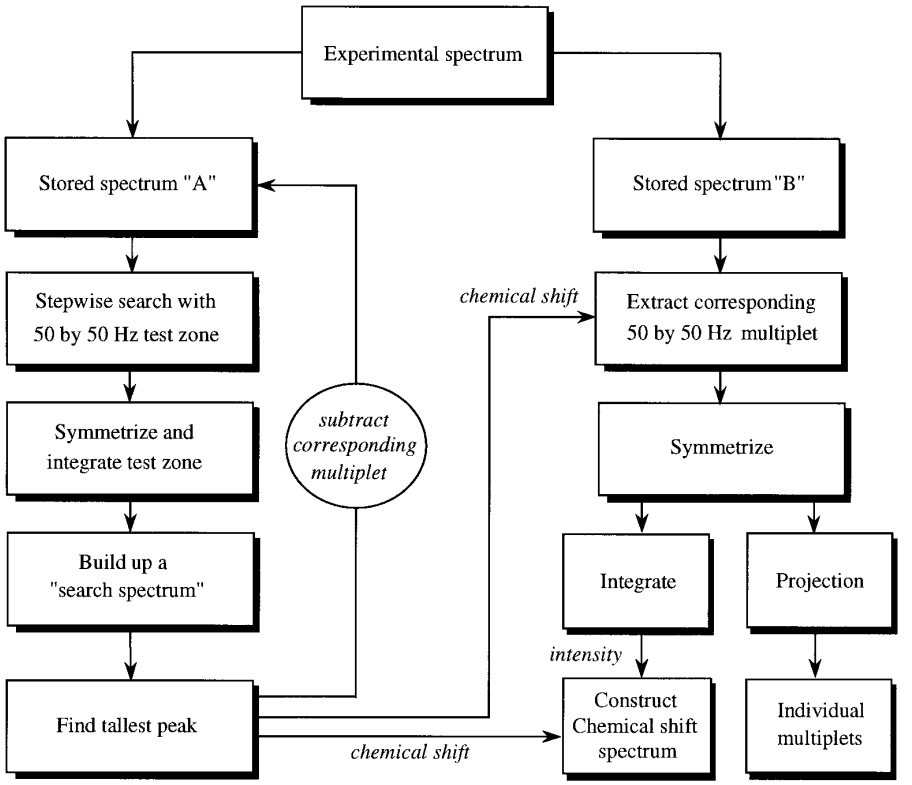

FIG. 5. Schematic flow chart of the program to extract chemical shifts and individual spin-multiplet patterns. Note that a second copy ''B'' of the experimental spectrum is used for the final processing stage; this avoids cumulative errors arising from repeated subtraction.

with a reflected J spectrum, it has the disadvantage that the total intensity is distributed over a larger number of multiplet components, so the two-dimensional multiplet has a lower signal-to-noise ratio, but the full intensity is retrieved in the chemical-shift spectrum and in projections of the individual multiplets. However, the spectra suffer from some baseline distortion that may degrade the uniformity of intensities in the chemical-shift spectrum.

z-Filtered J Spectra

The third approach removes the undesirable $2I_xS_z$ terms by means of a z filter (*14*) with a variable duration τ to scramble the phases of zero- and multiple-quantum coherence:

$$90^\circ_{\phi_1}\text{—}\tfrac{1}{2}t_1\text{—}180^\circ_{\phi_2}\text{—}\tfrac{1}{2}t_1\text{—}90^\circ_{\phi_3}\text{—}\tau\text{—}90^\circ_{\phi_4}\text{—acquire}_{\phi_5}$$

$$\begin{array}{lllll} \phi_1 & 0 & 0 & 0 & 0 \\ \phi_2 & 0 & 1 & 2 & 3 \\ \phi_3 & 0 & 0 & 0 & 0 \\ \phi_4 & 0 & 0 & 0 & 0 \\ \phi_5 & 0 & 2 & 0 & 2 \end{array} \qquad [3]$$

The z filter stores the magnetization of interest along the $\pm z$ axis, using different storage times so that the undesirable coherences cancel. Typically eight values of τ would be employed (for example, 20, 4, 15, 10, 12, 30, 7, 27 ms). Figure 3 illustrates how the progressive introduction of more τ values gradually converts a typical two-dimensional multiplet pattern from the ''diagonal'' form of Fig. 3a to the square array shown in Fig. 3e.

The z-filter scheme is rather simpler to implement than the magic-angle purging technique but requires a more protracted signal accumulation to accommodate the set of τ values. It has the important advantage that the undesirable product-operator terms are effectively suppressed, giving two-dimensional multiplets where all the component lines are in pure absorption and have the same intensity. This allows the individual one-dimensional multiplets to be obtained either by projection or by taking suitable sections parallel to the F_1 or F_2 axis.

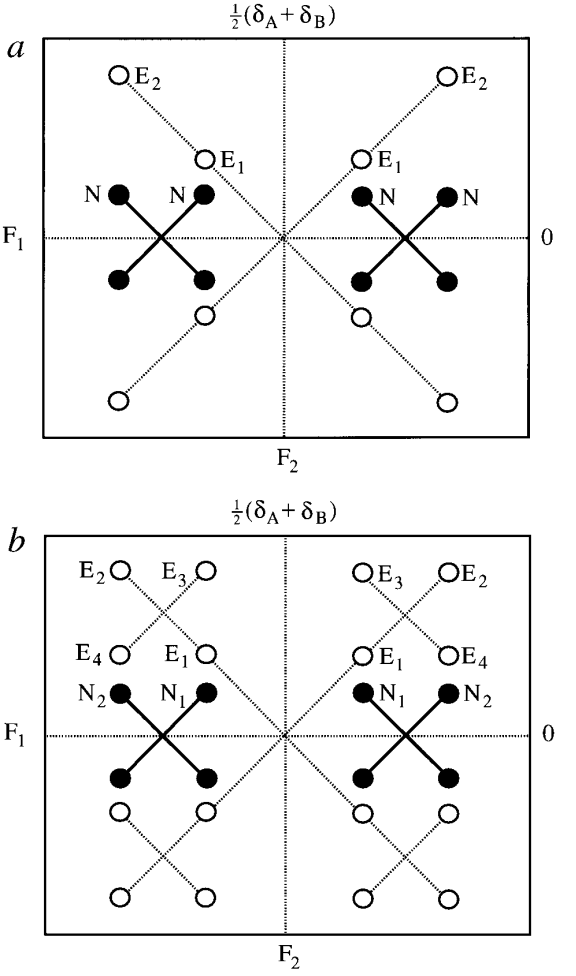

FIG. 6. Schematic diagram of a reflected J spectrum (a) and a z-filtered J spectrum (b) from an AB spin system with $\delta_A - \delta_B = 8.0$ Hz and $J = 3.0$ Hz, giving $\tan 2\theta = 0.375$. The ''normal'' lines are represented by filled circles and the ''extraordinary'' lines by open circles. The spectra are exactly symmetrical with respect to reflection in the axis $F_1 = 0$. General expressions for the frequencies and intensities are given in Table 1.

SYMMETRIZATION

All three methods employ the same symmetry algorithm (PROSIT, available on request). The experimental two-dimensional J spectrum is in the form of a long thin strip, approximately 50 Hz wide (F_1) and 10 ppm long (F_2). We first store two separate copies of the raw experimental spectrum (A and B) for reasons explained below. Separation of interpenetrating multiplets is achieved by a pattern-recognition algorithm based on symmetry. In all three modes of this experiment there is exact reflection symmetry about the axis $F_1 = 0$ for both signals and noise. For weakly coupled spectra, there is also a point at the center of each individual spin multiplet about which there is C_{4v} symmetry. This symmetry center is taken to be the chemical shift.

Ideally, the ordinates at eight symmetrically related locations surrounding such a symmetry center have identical intensities (Fig. 4a), but four of these locations with positive F_1 frequencies have *exactly* the same intensities (including noise) as the corresponding four with negative F_1 frequencies. The test routine therefore focuses on the former four locations (Fig. 4b). A schematic flow chart of this operation is shown in Fig. 5.

In an initial search mode, a square test zone (usually 50 by 50 Hz) is moved step by step through the two-dimensional J

TABLE 1
Frequencies and Intensities in *J* Spectra for the AB Case[a]

Peak	F_1 (Hz)	F_2 (Hz)	Intensity
		Reflected *J* spectrum	
N	$\pm\frac{1}{2}J$	$\frac{1}{2}(\delta_A + \delta_B) \pm (D \pm \frac{1}{2}J)$	$+\frac{1}{4}\cos^2 2\theta$
E_1	$\pm(D - \frac{1}{2}J)$	$\frac{1}{2}(\delta_A + \delta_B) \pm (D - \frac{1}{2}J)$	$+\frac{1}{4}\sin 2\theta(1 + \sin 2\theta)$
E_2	$\pm(D + \frac{1}{2}J)$	$\frac{1}{2}(\delta_A + \delta_B) \pm (D + \frac{1}{2}J)$	$-\frac{1}{4}\sin 2\theta(1 - \sin 2\theta)$
		z-filtered *J* spectrum	
N_1	$\pm\frac{1}{2}J$	$\frac{1}{2}(\delta_A + \delta_B) \pm (D - \frac{1}{2}J)$	$+\frac{1}{4}(1 + \sin 2\theta)\cos^2 2\theta$
N_2	$\pm\frac{1}{2}J$	$\frac{1}{2}(\delta_A + \delta_B) \pm (D + \frac{1}{2}J)$	$+\frac{1}{4}(1 - \sin 2\theta)\cos^2 2\theta$
E_1	$\pm(D - \frac{1}{2}J)$	$\frac{1}{2}(\delta_A + \delta_B) \pm (D - \frac{1}{2}J)$	$+\frac{1}{8}\sin 2\theta(1 + \sin 2\,\theta)^2$
E_2	$\pm(D + \frac{1}{2}J)$	$\frac{1}{2}(\delta_A + \delta_B) \pm (D + \frac{1}{2}J)$	$-\frac{1}{8}\sin 2\theta(1 - \sin 2\,\theta)^2$
E_3	$\pm(D + \frac{1}{2}J)$	$\frac{1}{2}(\delta_A + \delta_B) \pm (D - \frac{1}{2}J)$	$-\frac{1}{8}\sin 2\theta\cos^2 2\theta$
E_4	$\pm(D - \frac{1}{2}J)$	$\frac{1}{2}(\delta_A + \delta_B) \pm (D + \frac{1}{2}J)$	$+\frac{1}{8}\sin 2\theta\cos^2 2\theta$

After symmetrization, integration, and projection onto the F_2 axis

Peak	F_2 (Hz)	Reflected *J* spectrum intensity	*z*-filtered *J* spectrum intensity
A line	$\frac{1}{2}(\delta_A + \delta_B) + D$	$+\cos^2 2\theta$	$+(1 - \sin 2\theta)\cos^2 2\theta$
B line	$\frac{1}{2}(\delta_A + \delta_B) - D$	$+\cos^2 2\theta$	$+(1 - \sin 2\theta)\cos^2 2\theta$
Extra	$\frac{1}{2}(\delta_A + \delta_B)$	$+2\sin^2 2\theta$	$+2\sin^2 2\theta$

[a] With the definitions $2D = [(\delta_A - \delta_B)^2 + J^2]^{1/2}$ and $\tan 2\theta = J_{AB}/(\delta_A - \delta_B)$.

spectrum, and, at each increment of F_2, the entire zone is processed to enforce the required symmetry. In the present work we have employed a simpler algorithm than the one described earlier (*11*). The symmetry filter used is not based on strict C_{4v} symmetry, because under conditions of strong coupling, certain lines can have negative intensities (see below) and only the magnitudes satisfy a C_{4v} symmetry test. The symmetrization procedure compares the moduli of the intensities at each of the four locations shown in Fig. 4b and replaces them all by the lowest value, retaining the original signs. The same value is placed in the corresponding four locations at negative F_1 values. The process is repeated until the entire 50 by 50 Hz test zone has been symmetrized.

This is a powerful means for suppressing signals that do not possess the correct symmetry, and, in particular, for the rejection of overlapping responses from any adjacent multiplets. When different levels of sophistication were introduced into the symmetrization algorithm, for example, the use of the arithmetic mean rather than the lowest value, or correction for abnormally high or low intensities, the results were judged to be worse or at least no better, and these refinements were therefore abandoned. After symmetrization, the integral over the test zone is assigned to the intensity of a singlet at the center of symmetry. This is assumed to be the chemical shift of that particular site, although in the case of strong coupling, there will be a slight frequency displacement. In order to construct a realistic chemical-shift spectrum by projection onto the F_2 axis, this singlet is assigned a suitable Lorentzian lineshape.

The first complete pass through the two-dimensional *J* spectrum in the F_2 direction generates a one-dimensional ''search spectrum'' which consists of peaks at each apparent center of symmetry. Some of these peaks are ''false'' in the sense that they arise from accidental symmetry between lines from adjacent multiplets. In order to attenuate these overlap effects, the tallest peak in the search spectrum is selected, and the corresponding two-dimensional multiplet is subtracted from the stored spectrum ''A''. This removes contributions of this multiplet to the spectrum of its immediate neighbors. (It also provides a measure of the first proton chemical shift, which is then used to begin construction of chemical-shift spectrum.) The process is then repeated on the modified spectrum ''A'', generating a second search spectrum from which we subtract the next tallest peak. By progressively selecting the tallest remaining peak, and subtracting spin multiplets one at a time, overlap effects are minimized (*8*). There may still be some residual ''accidental'' centers of symmetry, but they are relatively weak. This iteration is terminated just before the remaining peaks in the search spectrum approach a predetermined threshold level (usually 5% of the height of a methyl resonance), or at a point where the expected number of chemically distinct sites

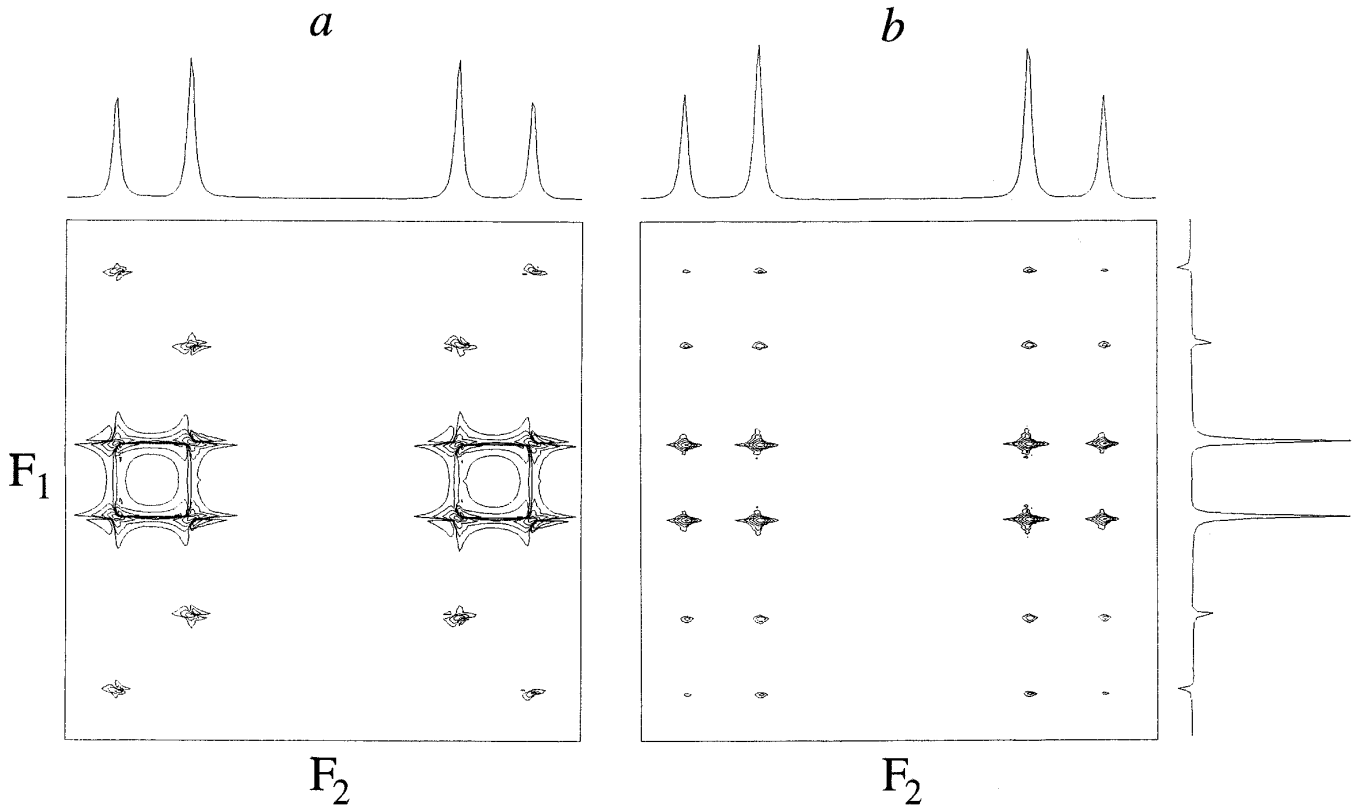

FIG. 7. Experimental *J* spectra of the AB spin system of protons in citric acid (110 by 110 Hz regions). (a) The reflected *J* spectrum, with 8 normal lines in a square pattern and 8 extraordinary lines, all with the phase-twist lineshape. (b) The *z*-filtered *J* spectrum, with 8 normal lines and 16 extraordinary lines, all with pure absorption lineshapes. The outermost extraordinary lines (in the F_1 dimension) have negative intensities, as seen in the F_1 projection of (b). Both types of spectrum give the familiar AB pattern in the F_2 projection (top).

has already been determined. Errors of judgment at this stage may lead to genuine chemical shifts being overlooked or to the detection of spurious peaks in the chemical-shift spectrum. However, we have found that a false peak can usually be recognized because the corresponding two-dimensional multiplet has an anomalous structure, quite different from the familiar patterns.

Symmetrization slightly perturbs the original intensities of the multiplets through strong-coupling effects and accidental overlap. Consequently there are cumulative errors in the repeated subtraction of symmetrized two-dimensional multiplets from the stored spectrum ''A''. For this reason, the chemical-shift spectrum utilizes intensities derived from copy ''B'', using the chemical-shift value determined from the current search spectrum. The subtraction process applied to spectrum ''B'' is *not* cumulative, and therefore gives more reliable values for the relative intensities.

The intensity is the integral calculated over the appropriate 50 by 50 Hz test zone, after symmetrization. In the ideal case, each chemically distinct site would have the same intensity (after making allowance for chemical equivalence), but in practice the integral may be too high if overlap effects are not completely eliminated, or too low if there are strong-coupling effects. The corresponding spin-multiplet structure is a projection onto the F_2 axis (or a suitable section parallel to F_2).

STRONG-COUPLING EFFECTS

Strong coupling is always a problem when we try to analyze a high-resolution spectrum by inspection. The same is true of two-dimensional *J* spectroscopy. It has been shown (*15–18*) that even in the simplest case of an AB spectrum, strong coupling introduces new transitions into the F_1 dimension of a two-dimensional *J* spectrum. They are the previously forbidden zero- and double-quantum transitions, the latter having negative intensity (*16*, *17*).

The Reflected J Spectrum of an AB System

We adopt the standard definitions

$$\tan 2\theta = J/(\delta_A - \delta_B) \qquad [4]$$

and the positive quantity D defined by

$$2D = [(\delta_A - \delta_B)^2 + J^2]^{1/2}. \qquad [5]$$

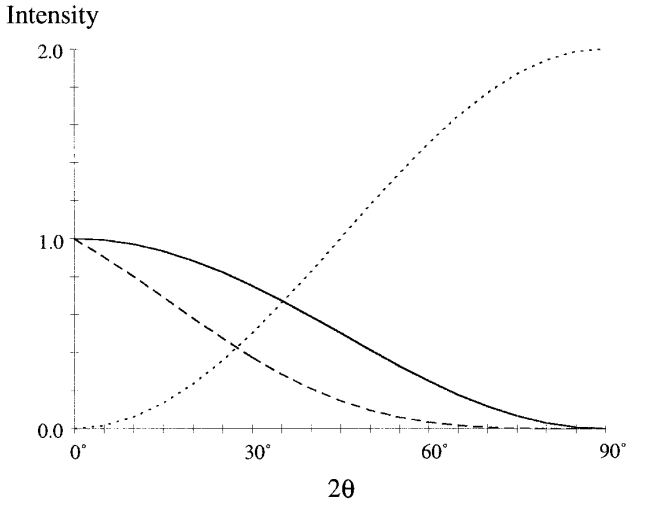

FIG. 8. The relative intensities of the ''normal'' and ''extraordinary'' lines calculated for an AB chemical-shift spectrum, plotted as a function of the strong-coupling parameter, $2\theta = \arctan[J_{AB}/(\delta_A - \delta_B)]$. Full curve: normal lines from a reflected *J* spectrum. Dashed curve: normal lines from a purged or *z*-filtered spectrum. Dotted curve: extraordinary lines. See Table 1.

We may divide the *J* spectrum into ''normal'' lines (those that would be observed in the weakly coupled case) and ''extraordinary'' lines (those that only appear when there is strong coupling). The normal lines (N) form two St. Andrew's crosses with centers of symmetry at F_2 frequencies $\frac{1}{2}(\delta_A + \delta_B) \pm D$ (Fig. 6a). Note that they all have the same intensity, and no intensity is lost on symmetrization (Table 1).

The eight ''extraordinary'' lines (labeled E_1 and E_2) form another St. Andrew's cross centered at the mean chemical shift $\frac{1}{2}(\delta_A + \delta_B)$ in the F_2 dimension. The coordinates and intensities are set out in Table 1. We restrict our consideration to the absorption components, on the grounds that in the later integration step, the dispersion contributions cancel. The outer lines (E_2) have a negative intensity, and they may in practice be aliased if the F_1 spectral width is too narrow. It is interesting to note that it is the contributions from E_1 and E_2 that give rise to the familiar ''tent effect'' on the intensities of the conventional AB spectrum (the projection on the F_2 axis). The integral of these eight extraordinary lines over a suitably wide test zone is $+2 \sin^2 2\theta$.

An experimental illustration of a reflected *J* spectrum of an AB system is provided by the 400 MHz proton spectrum of citric acid (Fig. 7a), which has $\tan 2\theta = 0.22$. Note the phase-twist lineshapes. The extraordinary lines form a St. Andrew's cross centered at the mean chemical shift $\frac{1}{2}(\delta_A + \delta_B)$. The eight normal lines all have the same intensity but the contributions from the extraordinary lines create the familiar ''tent effect'' when the intensities are projected onto the F_2 axis.

Purged and z-Filtered J Spectra of an AB System

The purged *J* spectrum and the *z*-filtered *J* spectrum of an AB spin system are predicted to have the same structure (Fig. 6b). The ''normal'' lines still form two St. Andrew's crosses separated by $2D$ in the F_2 dimension, but now the outer lines (N_2) are weaker than the ''inner'' lines (N_1) as indicated in Table 1. After symmetrization, the lowest value algorithm reduces the intensity of the normal transitions by a factor $(1 - \sin 2\theta)$, compared with the corresponding reflected *J* spectrum.

There are 16 extraordinary lines with intensities E_1, E_2, E_3, and E_4 (Table 1). Note that the outermost lines in the F_1 dimension (E_2 and E_3) have negative intensities. The intensities of E_3 and E_4 are equal and opposite in sign, and their contribution to the total integral vanishes. After symmetrization and collection of the integrated intensity into a singlet at the center of symmetry, the extraordinary response at $\frac{1}{2}(\delta_A + \delta_B)$ has the same relative intensity $(2 \sin^2 2\theta)$ as that calculated for the reflected *J* spectrum. Clearly, as the coupling becomes stronger, the extraordinary response at $\frac{1}{2}(\delta_A + \delta_B)$ gains in intensity at the expense of the normal responses at $\frac{1}{2}(\delta_A + \delta_B) \pm D$, and in the limit we observe only the mean chemical shift. A graph of the relative intensities as a function of the strong-coupling parameter 2θ is shown in Fig. 8. For a chemical-shift spectrum derived from a purged or *z*-filtered *J* spectrum, the intensity of the extraordinary line begins to exceed that of the two normal lines when $|J_{AB}|$ exceeds $0.52\ |\delta_A - \delta_B|$.

The *z*-filtered *J* spectrum of citric acid is shown in Fig. 7b, illustrating the 16 extraordinary lines sketched out in Fig. 6b. Note the pure absorption lineshapes. The intensities of the normal lines (N_1 and N_2) now exhibit the familiar ''tenting'' effect characteristic of one-dimensional AB spectra. The projection onto the F_1 axis clearly shows that the outer lines E_2 and E_3 have negative intensities.

ABX and Higher Spin Systems

This analysis is readily extended to the ABX case since the strongly coupled region can be factored into two AB subspectra, one for X spins in an α state and the other for X spins in a β state. This gives the *effective* chemical shifts:

$$(\delta_A + \tfrac{1}{2}J_{AX}) \quad \text{and} \quad (\delta_B + \tfrac{1}{2}J_{BX}) \qquad [6]$$

$$(\delta_A - \tfrac{1}{2}J_{AX}) \quad \text{and} \quad (\delta_B - \tfrac{1}{2}J_{BX}). \qquad [7]$$

We now believe that strong coupling led to an error in our initial analysis (*11*) of the proton reflected *J* spectrum of 4-androsten-3,17-dione. Two spurious peaks were found at approximately 2.37 and 2.39 ppm; these are in fact the symmetry centers of the extraordinary lines of an ABX spin system (complicated by some further small couplings). In addition, two genuine peaks were missed, owing to near

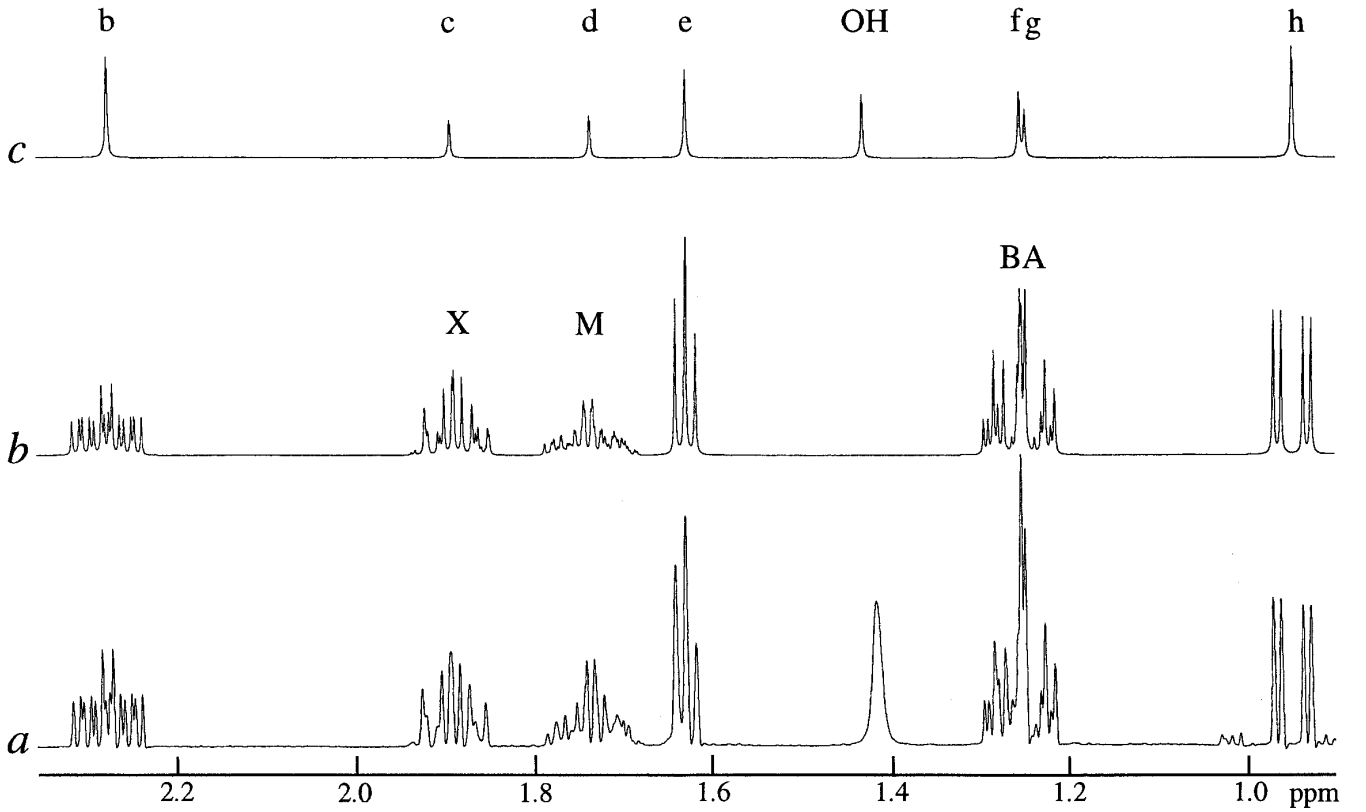

FIG. 9. (a) The conventional 400 MHz spectrum of borneol in $CDCl_3$. (b) The corresponding simulated spectrum. (c) The chemical-shift spectrum. Attention is focused on the ABMX strongly coupled spin system (see Table 2) which gives anomalously low decoupled intensities for protons M and X.

degeneracies, one at 2.43 ppm (separation 0.004 ppm) and another at 1.97 ppm (separation 0.004 ppm). The present work now provides convincing evidence for this reassignment, corroborated by determination of the integrals.

Many practical situations involve spin systems that are more complicated, and in these more general cases, the component lines of a spin multiplet are not necessarily exactly symmetrically disposed in frequency. This interferes with the symmetrization procedure and leads to an additional loss of intensity. A case in point is provided by the experimental *z*-filtered proton *J* spectrum of borneol (*19*). The conventional 400 MHz spectrum in $CDCl_3$ is shown in Fig. 9 and is compared with a computer simulation based on the observed chemical shifts and manual refining of the coupling constants. The strongly coupled protons of interest form an ABMX spin system with some first-order couplings to further protons outside the ABMX group. The relevant coupling constants and chemical-shift differences are listed in Table 2. Strong coupling degrades the symmetry, particularly for the M multiplet which is appreciably distorted (Fig. 10a), and, when the symmetrization algorithm is applied (Fig. 10b), there is a considerable loss of intensity due to the frequency displacements.

We conclude that *J* spectra of strongly coupled protons exhibit the same kinds of problems that are encountered in conventional high-resolution spectroscopy—frequency displacements and intensity distortions within spin multiplets. The program indicates a ''chemical shift'' at the center of each symmetrized multiplet, not the true chemical shift. This is the same discrepancy that occurs in conventional one-dimensional spectroscopy of an AB spin system; we observe $2D$ rather than $(\delta_A - \delta_B)$ for the apparent chemical shift. There is also the added complication of additional responses centered on the mean chemical shift of strongly coupled pairs of spins. Fortunately, at present-day magnetic field

TABLE 2
Chemical Shifts and Coupling Constants for the ABMX Spin System in Borneol[a]

ν_A = 0.0 Hz	J_{AB} = +4.4 Hz
ν_B = 2.2 Hz	J_{AM} = −13.0 Hz
ν_M = 195.6 Hz	J_{AX} = +9.5 Hz
ν_X = 256.4 Hz	J_{BM} = +12.3 Hz
	J_{BX} = −13.2 Hz
$\lvert J_{AB}/(\nu_A - \nu_B)\rvert$ = 2.0	J_{MX} = +4.4 Hz

[a] Estimated error ± 0.4 Hz.

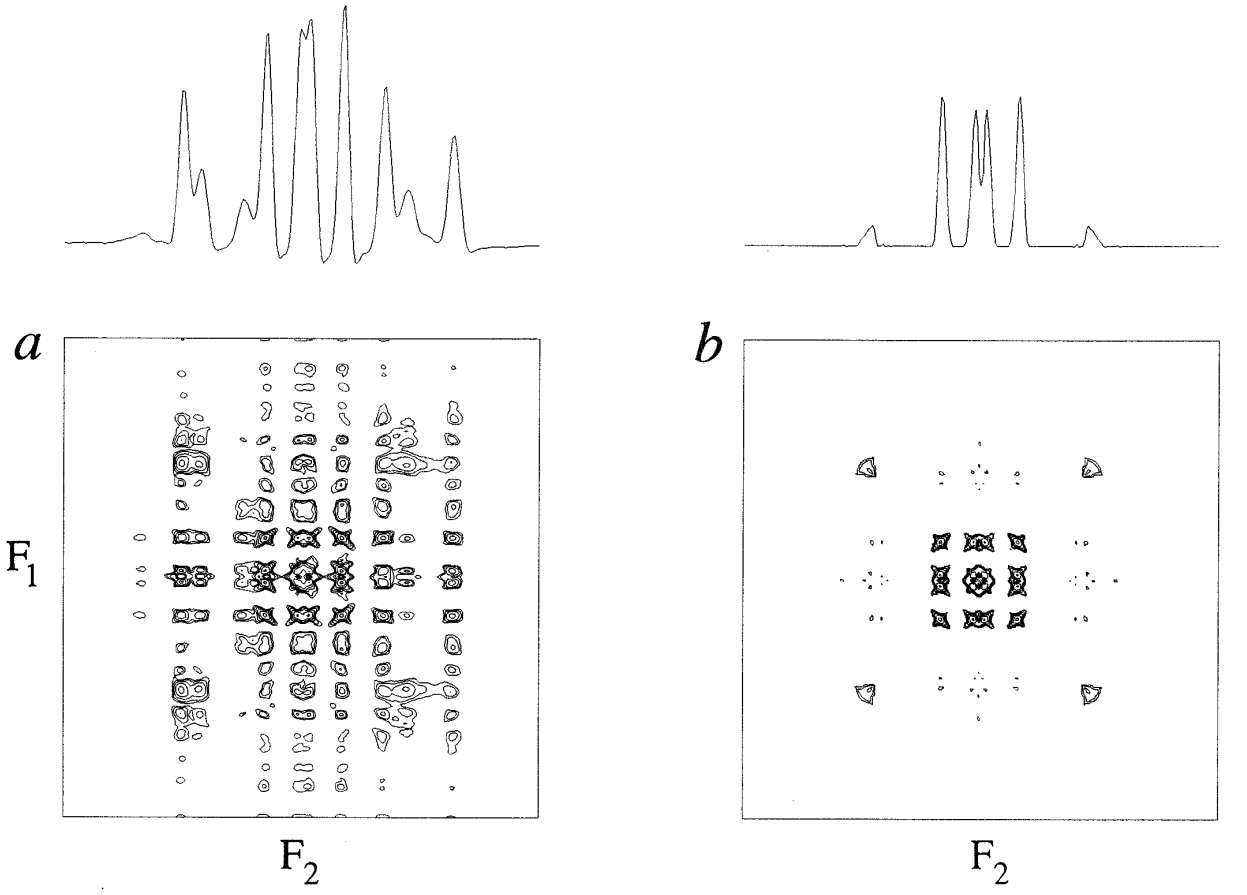

FIG. 10. The 40 × 40 Hz two-dimensional spin multiplet from the *z*-filtered *J* spectrum of proton M of borneol. (a) Strong coupling not only affects relative intensities but also slightly distorts the C_{4v} symmetry of the frequencies. (b) Consequently the symmetry filter appreciably attenuates this multiplet. The integral projections are shown along the top margin.

strengths, instances of very strongly coupled spin systems are relatively rare.

EXPERIMENTAL

Measurements were carried out on a Varian VXR-400 spectrometer. It was found that efficient separation of multiplets with the symmetry filter required a good signal-to-noise ratio and high-resolution conditions. Typically the experimental linewidths (spinning sample) were between 1.0 and 1.6 Hz, and resolution enhancement was applied in both frequency dimensions, giving a final linewidth of between 0.6 and 1.2 Hz, with at least four data points per hertz. Poor resolution was found to lead to artifacts in the processed spectrum, particularly for overlapped multiplets.

RESULTS

The conventional spectrum of 4-androsten-3,17-dione is shown in Fig. 11, along with the molecular structure and the assignment. Chemical shifts and coupling constants are set out in Table 3. We focus attention on the most serious overlap problems, which occur in the regions between 2.28 and 2.54 ppm and between 1.92 and 2.16 ppm. This is where the misassignment was made in our earlier publication (*11*). The present analysis and an evaluation of the integrals strongly suggest that these regions consist of groups of resonances arising from five protons and four protons, respectively, in contrast to our earlier finding.

J spectra from the 1.92 to 2.54 ppm region were recorded by the three different experimental techniques. Figure 12a shows the reflected *J* spectrum, where the sparse nature of the basic multiplet pattern might appear to offer a better chance of separating the overlapping responses. However, the phase-twist lineshape militates against this, with the result that this proves to be rather less successful than the other two methods for obtaining decoupled proton spectra.

Figure 12b shows the same section of the *J* spectrum purged by means of the scheme sketched in Fig. 2, with a period of 25 ms locked along an effective field tilted at the magic angle. This spectrum should resemble that of Fig. 12c, obtained by the use of a *z* filter, but in fact, although

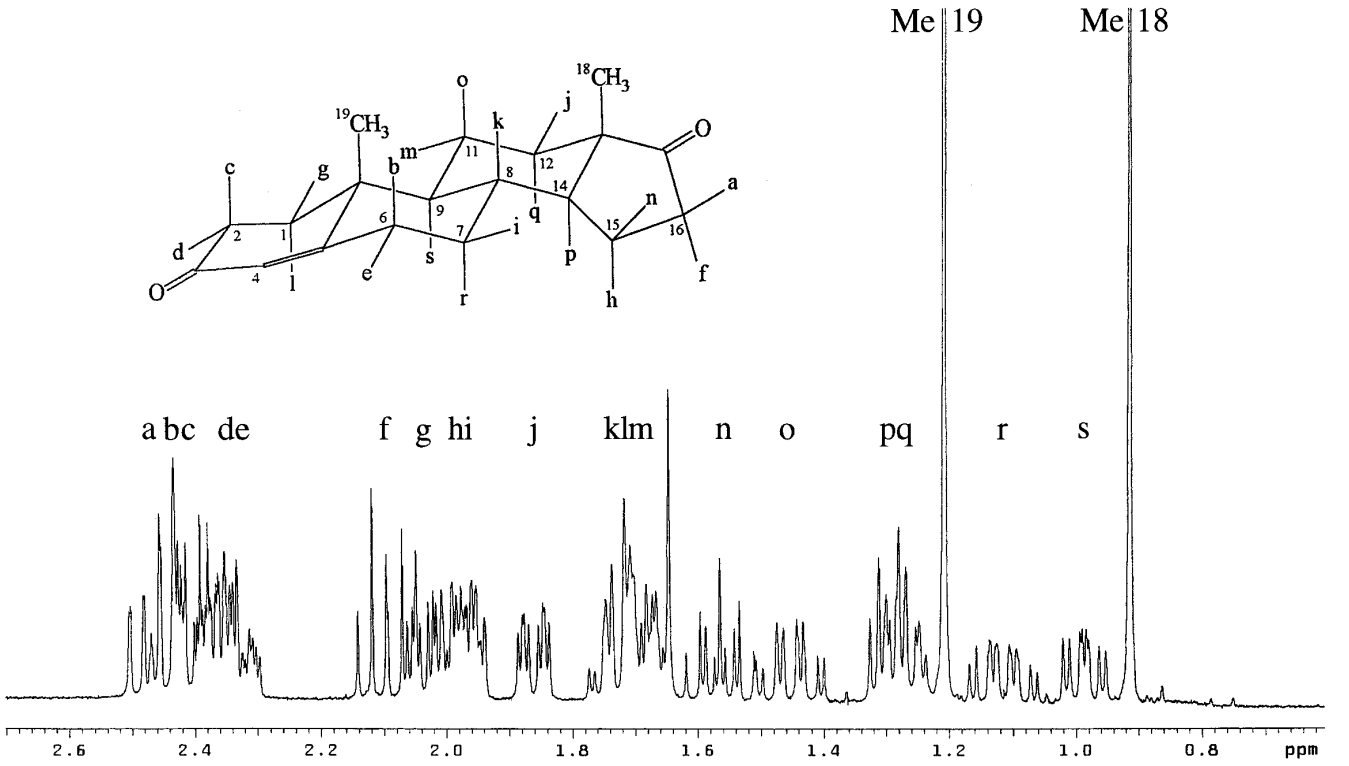

FIG. 11. Part of the conventional 400 MHz proton spectrum of 4-androsten-3,17-dione together with the assignment of the resonances. The two methyl resonances have been truncated.

TABLE 3
Chemical Shifts[a] and Coupling Constants[a] for 4-Androsten-3,17-dione in $CDCl_3$

Label	Proton	Shift (ppm)[b]	Coupling constants (Hz)[c]
a	16β	2.464	19.3 (f), 9.1 (n), 1.0 (h)
b	6β	2.423	14.6 (e), 13.7 (r), 5.2 (i), 1.8 (H-4)
c	2β	2.419	16.9 (d), 13.9 (l), 5.0 (g)
d	2α	2.338	16.9 (c), 5.4 (1), 3.5 (g), 0.9 (H-4)
e	6α	2.318	14.6 (b), 4.5 (r), 2.5 (i)
f	16α	2.090	19.3 (a), 9.1 (n), 8.9 (h)
g	1β	2.031	13.5 (l), 5.0 (c), 3.5 (d)
h	15α	1.967	12.3 (n), 8.9 (f), 5.9 (p), 1.0 (a)
i	7β	1.964	13.0 (r), 5.2 (b), 3.6 (k), 2.5 (e)
j	12β	1.856	12.9 (q), 4.2 (o), 2.7 (m)
k	8	1.722	11.7 (r), 10.8 (p), 10.7 (s), 3.6 (i)
l	1α	1.704	13.9 (c), 13.5 (g), 5.4 (d)
m	11α	1.681	13.8 (o), 4.2 (s), 4.0 (q), 2.7 (j)
n	15β	1.560	12.7 (p), 12.3 (h), 9.1 (a), 9.1 (f)
o	11β	1.448	13.8 (m), 12.4 (q), 12.4 (s), 4.2 (j)
p	14	1.284	12.7 (n), 10.8 (k), 5.9 (h)
q	12α	1.269	12.9 (j), 12.4 (o), 4.0 (m)
r	7α	1.109	13.7 (b), 13.0 (i), 11.7 (k), 4.5 (e)
s	9	0.980	12.4 (o), 10.7 (k), 4.2 (m)

[a] Based on a first-order analysis.
[b] Estimated error ± 0.001 ppm.
[c] Estimated error ± 0.4 Hz.

the basic structure is the same, the purging process leaves some small antiphase dispersion contributions on the baseline which distort the low-level contours. The cleanest result is undoubtedly from the *z*-filtered spectrum of Fig. 12c, where the basic symmetry of the two-dimensional multiplets is very clear. This was recorded by accumulating data for 16 different values of the τ parameter.

The decomposition of the congested region between 1.92 and 2.16 ppm into four separate two-dimensional multiplets is illustrated in Fig. 13. This emphasizes the power of the symmetry algorithm to extract a given two-dimensional multiplet from its overlapping neighbors. There is a clear indication of four proton resonances, two of which (h and i) have nearly degenerate frequencies (chemical-shift difference of only 0.004 ppm). These two multiplets are so tightly enmeshed that it is not possible to identify them by inspection.

A similar breakdown of the region between 2.28 and 2.52 ppm into five individual spin multiplets is shown in Fig. 14. The chemical shifts of two sites (b and c) are almost degenerate (separation 0.004 ppm) but are readily distinguished by the symmetry algorithm. There is considerable distortion of the intensities of the symmetrized multiplet from site d, attributed to the combination of accidental overlap of adjacent responses and strong coupling to site c with $J_{cd} = 16.9$ Hz and $(\delta_c - \delta_d) = 32.4$ Hz, giving $\tan 2\theta = 0.52$. The two-dimensional multiplet from site c is less distorted, probably

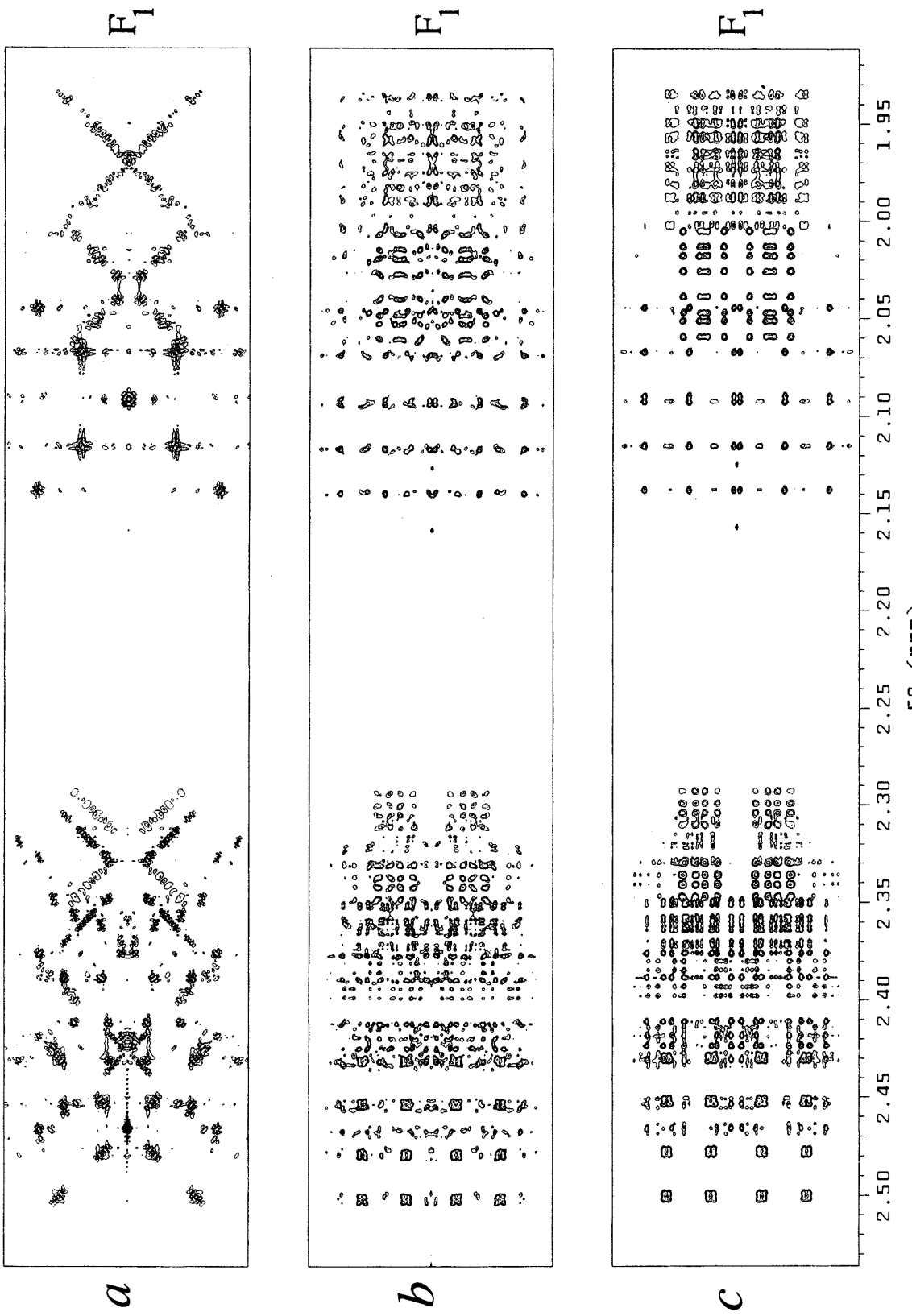

FIG. 12. A 50 Hz wide strip showing the congested region of the 400 MHz proton spectrum of 4-androsten-3,17-dione between 1.92 and 2.54 ppm, obtained (a) as a reflected *J* spectrum, (b) as a purged *J* spectrum, and (c) as a *z*-filtered *J* spectrum. In principle, spectra (b) and (c) should be very similar, but there are some baseline distortions in (b).

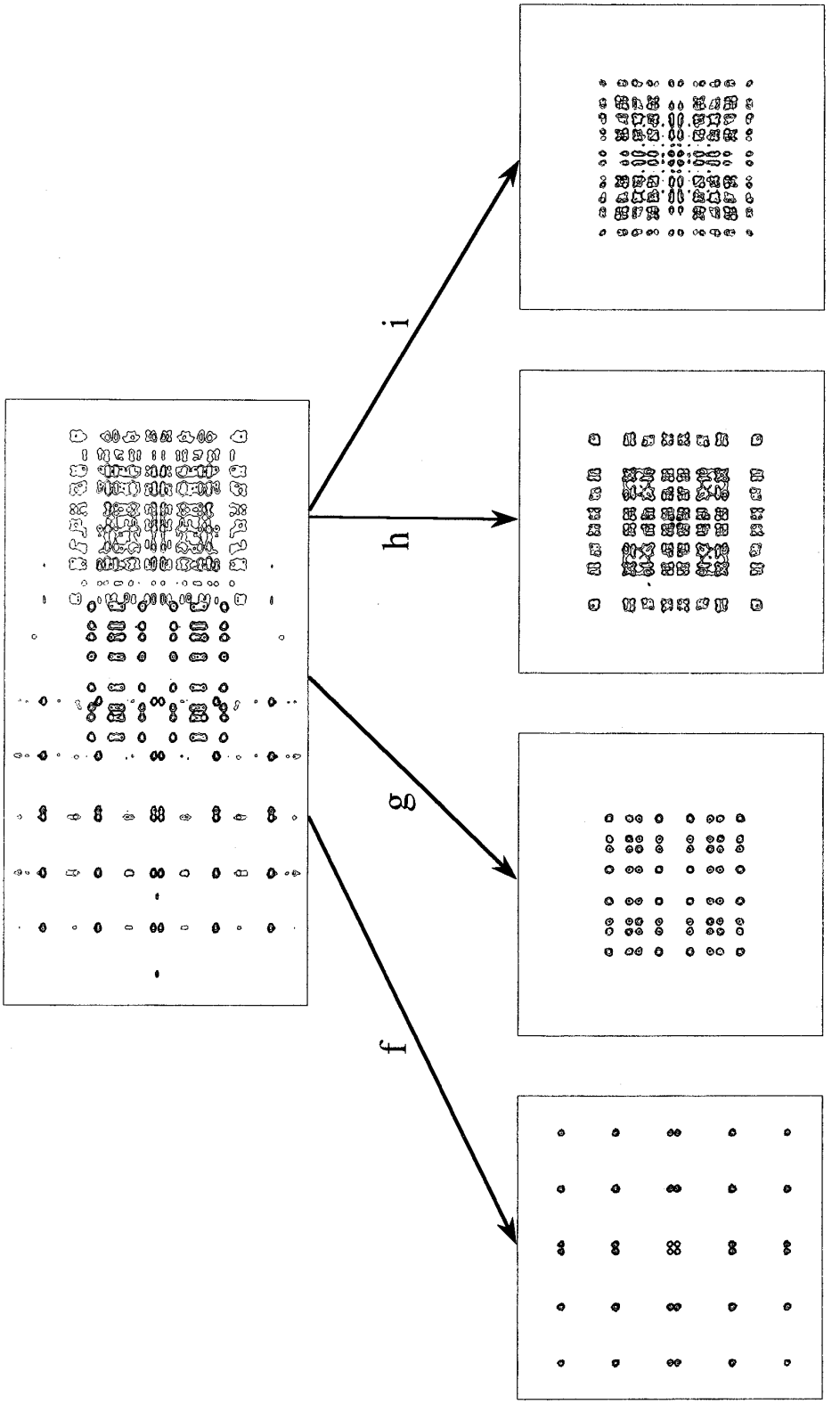

FIG. 13. Separation of four interpenetrating spin multiplets from the 1.92 to 2.16 region of the 4-androsten-3,17-dione spectrum into individual multiplets (50 by 50 Hz) by the symmetrization algorithm described in the text. Although two responses (h and i) have almost degenerate chemical shifts (0.004 ppm apart), the separation process is clearly very effective.

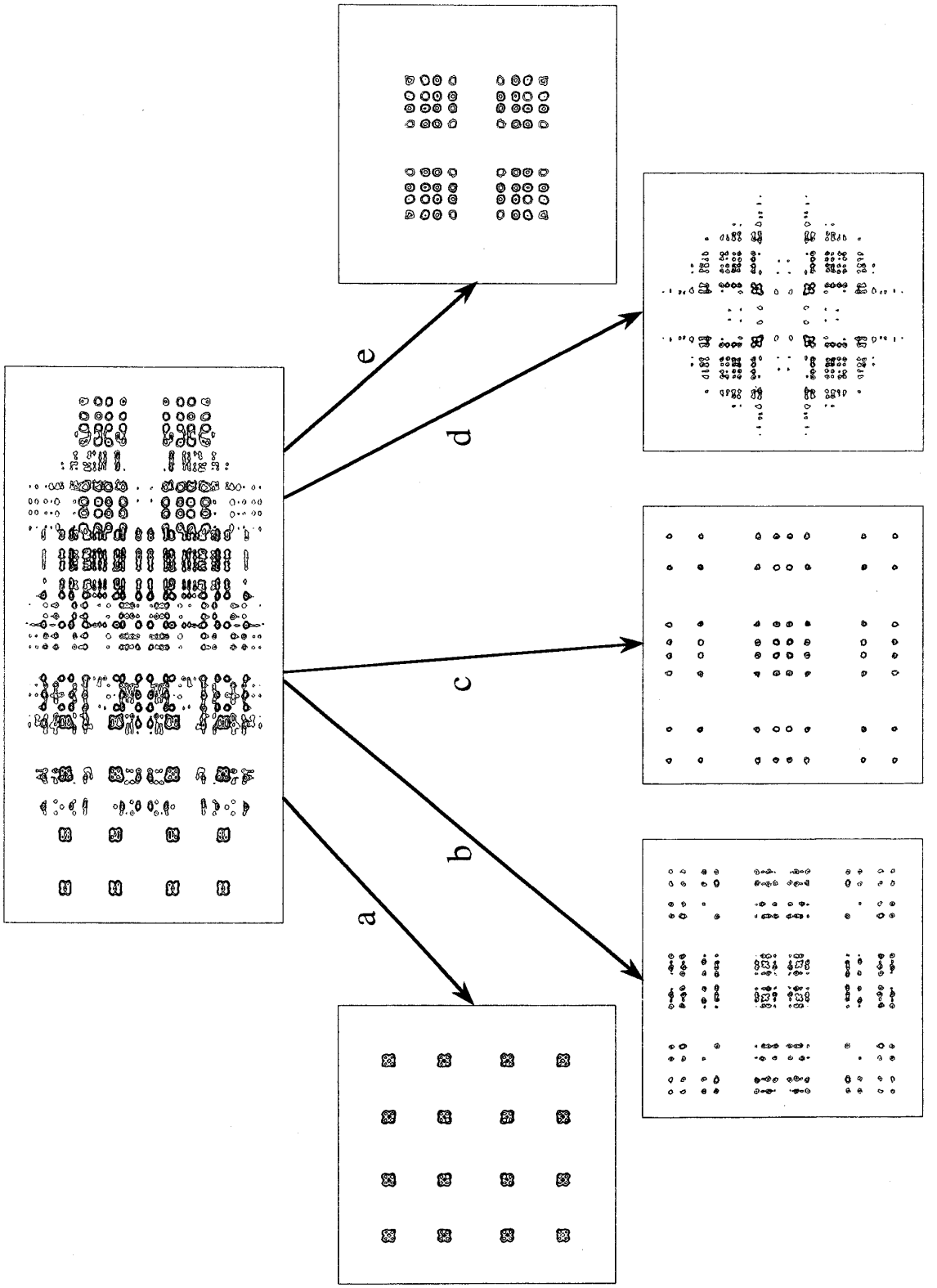

FIG. 14. Separation of five interpenetrating spin multiplets from the 2.28 to 2.52 ppm region of the 4-androsten-3,17-dione spectrum into individual multiplets (50 by 50 Hz). Two responses (b and c) have almost degenerate chemical shifts (0.004 ppm apart) but are cleanly separated by the symmetry filter. Multiplet (d) is distorted by the effects of accidental overlap and by strong coupling to proton c.

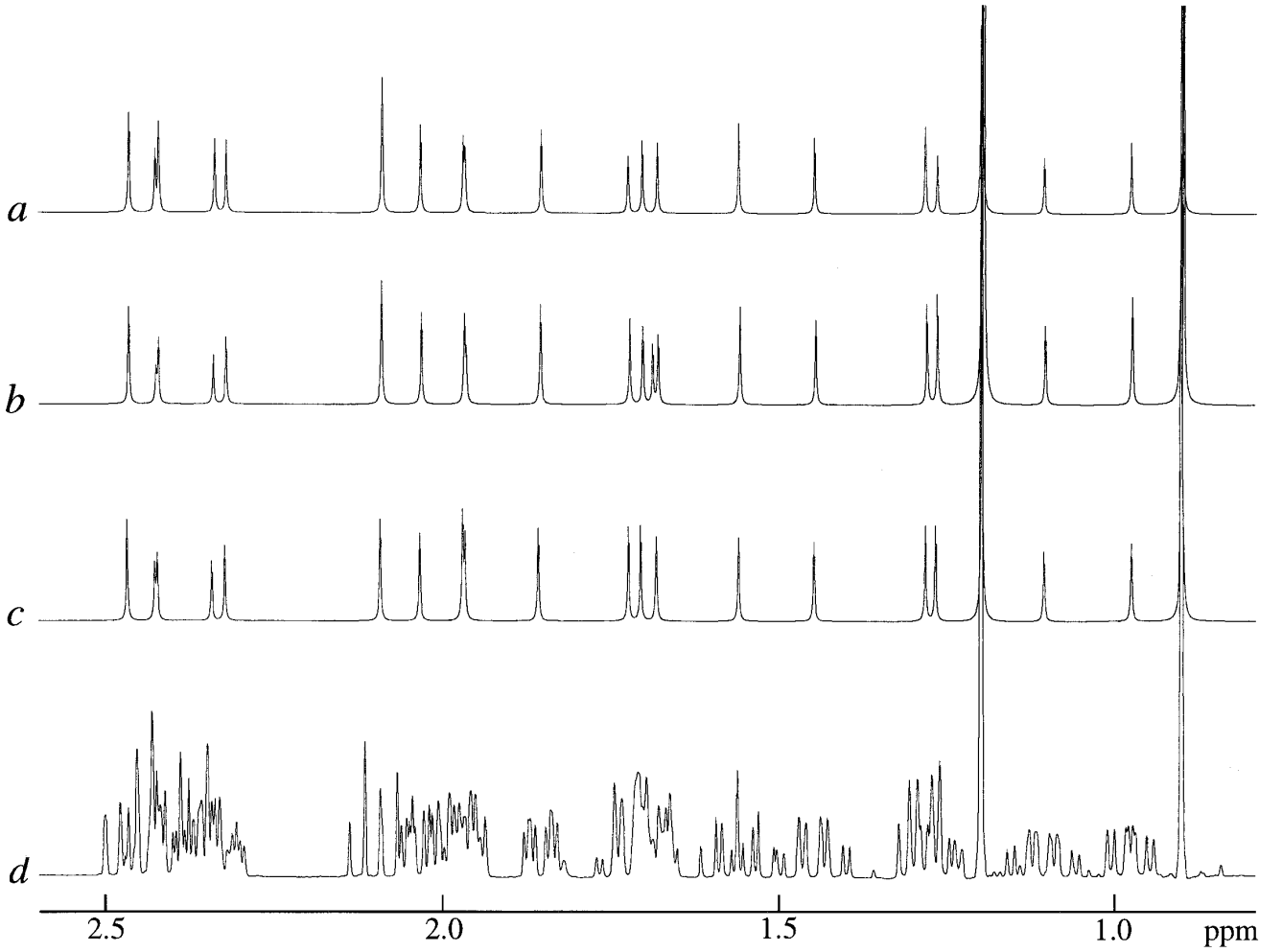

FIG. 15. Chemical-shift spectra of 4-androsten-3,17-dione obtained (a) from the reflected *J* spectrum, (b) from the purged *J* spectrum, and (c) from the *z*-filtered *J* spectrum. There is an additional response in (b) near 1.7 ppm from the residual water signal. The conventional spectrum (d) is included for comparison.

because there is less accidental overlap in that region. It was the existence of extraordinary lines from this strongly coupled pair of protons that gave rise to the incorrect assignment in our first analysis of this spectrum (*11*).

Once separation has been achieved, the centers of symmetry are taken as the chemical-shift values; there may be small errors here in the case of strongly coupled protons, but these are the same discrepancies that would occur in conventional spectroscopy without a proper analysis of the strongly coupled spin system. The computer routine reports the frequency of the symmetry centers to the nearest data point in the F_2 dimension; for display purposes these delta functions are converted into Lorentzian lines with a width commensurate with the instrumental linewidth in the coupled spectrum. Symmetrization and integration of a given separated multiplet give the relative intensity of that particular chemical site. Methyl group resonances were found to give unusually large integrals, significantly more than three times the intensity of single protons; this might be expected when using the lowest value algorithm on multiplets with a complicated structure.

Figure 15 shows the three different versions of the chemical-shift spectrum of 4-androsten-3,17-dione obtained by the three competing experimental methods; the conventional spectrum is also shown for comparison. All three decoupled spectra have the same structure as far as chemical shifts are concerned, but the intensities are not uniform, and the pattern of nonuniformity is not the same in the three cases. The residual variations in relative intensities are attributed partly to overlap and partly to strong-coupling effects. Probably the highest uniformity is achieved in the version obtained by *z* filtration (Fig. 15c). When the magic-angle locking scheme was used for purging, it was found that the choice of the locking period was rather critical. If it was too short or too long, then two strong-coupling artifacts were detected near 2.37 ppm; they disappeared when the locking period was around 25 ms. The purged spectrum also picks up a

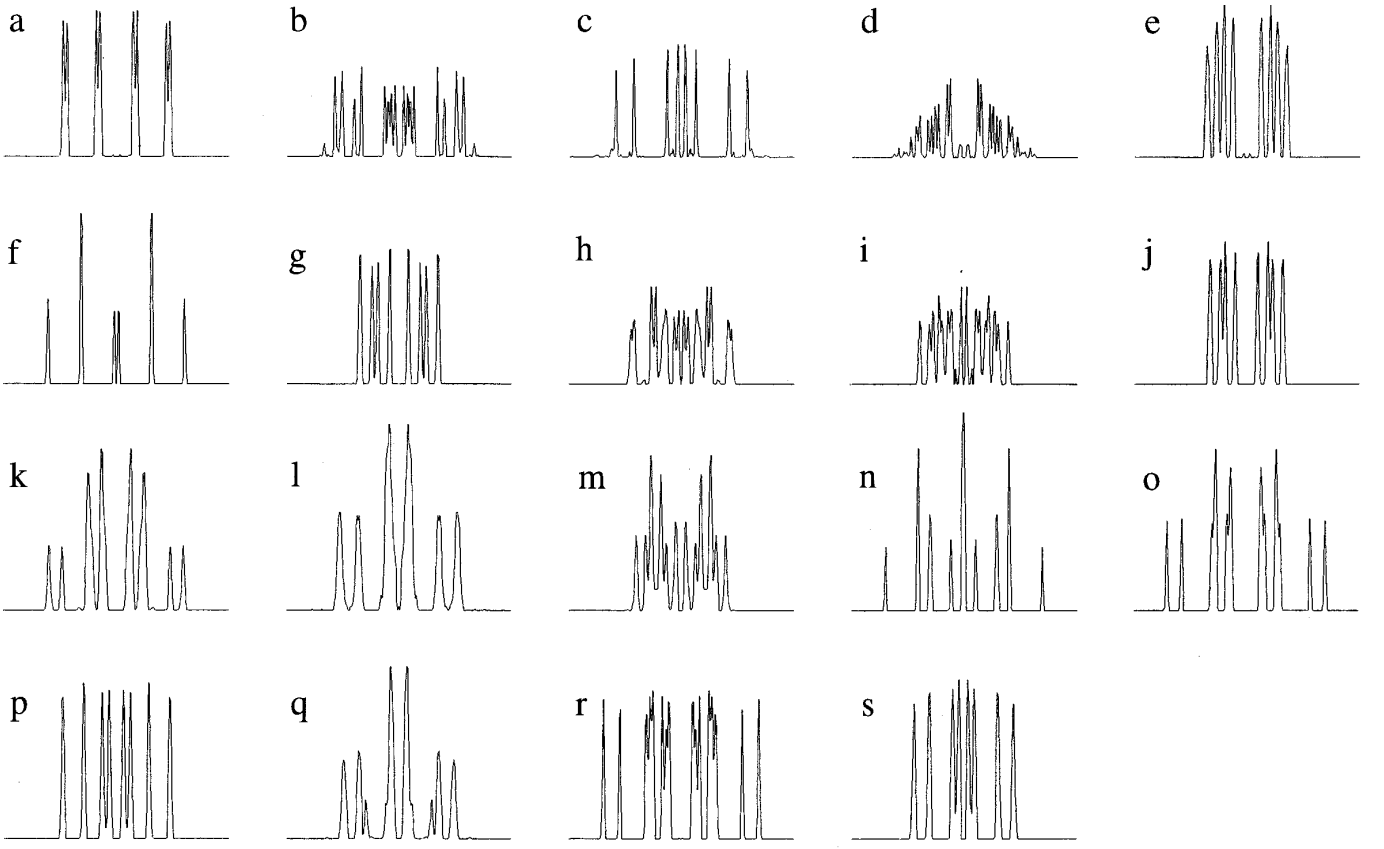

FIG. 16. Individual spin multiplets (62 Hz wide sections) from 19 chemically shifted sites in 4-androsten-3,17-dione obtained from the *z*-filtered *J* spectrum by symmetrization and projection onto the F_1 frequency axis. Note that the multiplet from site d shows appreciable intensity distortion attributed to accidental overlap and to strong-coupling effects.

weak response from residual water (near 1.7 ppm) that is missing in the other two schemes. This illustrates the main drawback of the adiabatic purging scheme—it requires care in setting up if the best results are to be obtained.

When all these considerations are taken into account, it seems clear that the *z*-filtration scheme is the most reliable—well worth the extra time it might take to acquire spectra at a set of different τ values. The dispersion-mode contributions to reflected *J* spectra are a nuisance because they have long tails in both frequency dimensions. The magic-angle locking method requires careful adjustment of the parameters for success.

Multiplet Structure

Not only do these new techniques provide a ''chemical-shift spectrum'' but also a spin multiplet from each chemically distinct site, essentially completely separated from its neighbors. These multiplets are of course exactly symmetrical at this stage. They can be used to extract the coupling constants by standard methods (see Table 3). Figure 16 displays spin multiplets from 19 proton sites of 4-androsten-3,17-dione. Note that the intensities within multiplets c and d show an appreciable distortion, particularly noticeable on the d multiplet. This is partly attributable to the operation of the symmetry filter on the *J* spectrum of the strongly coupled spin system ($\tan 2\theta = 0.52$), but this does not explain why the d multiplet is far more affected than that of proton c. The difference is attributed to the accidental overlap in the region of the d multiplet.

The symmetry algorithm is not entirely foolproof. Fortuitous symmetry patterns can occur when one complex two-dimensional multiplet encroaches on a neighbor, and these features pass through the symmetry filter. Fortunately the *z*-filtered *J* spectrum offers another approach to the separation of interpenetrating two-dimensional multiplets. Suitable sections through the experimental data often provide the required discrimination. Proton sites p and q of 4-androsten-3,17-dione are a case in point; we can see from Fig. 16 that the multiplet from site q has not been completely separated from its neighbor p by the symmetry filter. However, horizontal sections through the unprocessed experimental *J* spectrum at points a and b provide a much cleaner separation of the two multiplets in question (Fig. 17).

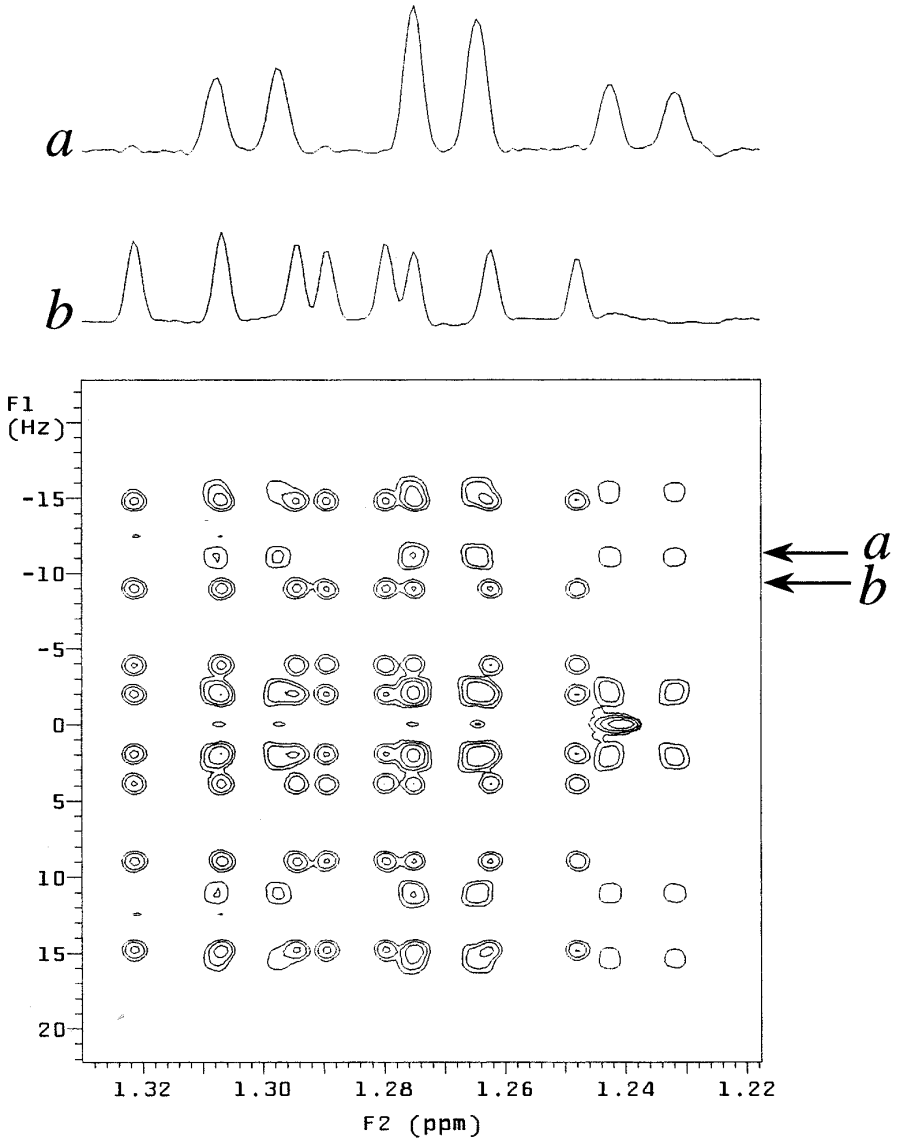

FIG. 17. Separation of individual spin multiplets (p and q) from the unprocessed 400 MHz *z*-filtered *J* spectrum of 4-androsten-3,17-dione by examining sections at (a) and (b). These may be compared with the corresponding results shown in Fig. 16, obtained by the symmetry algorithm.

CONCLUSIONS

Results obtained for 4-androsten-3,17-dione indicate that *J* spectroscopy can indeed provide acceptable chemical-shift spectra even in cases of severe overlap. The *z*-filtered technique seems to offer the best results in practice, although it involves the recording of several scans with different τ values. Complications arise from the accidental formation of symmetrical patterns from interpenetrating adjacent multiplets, but these are usually not serious. There are also perturbations from strong-coupling effects, mainly in the form of some loss of intensity and the appearance of ''extraordinary'' lines at the mean chemical shift.

ACKNOWLEDGMENTS

One of the authors (S.S.) thanks the Royal Society for financial support and another (H.S.) thanks the Österreichische Akademie der Wissenschaften.

REFERENCES

1. W. P. Aue, J. Karhan, and R. R. Ernst, *J. Chem. Phys.* **64,** 4226 (1976).
2. R. Freeman and H. D. W. Hill, *J. Chem. Phys.* **54,** 301 (1971).
3. G. Bodenhausen, R. Freeman, R. Niedermeyer, and D. L. Turner, *J. Magn. Reson.* **26,** 133 (1977).
4. K. Nagayama, P. Bachmann, K. Wüthrich, and R. R. Ernst, *J. Magn. Reson.* **31,** 133 (1978).

5. A. Bax, R. Freeman, and G. A. Morris, *J. Magn. Reson.* **43,** 333 (1981).

6. A. Bax and R. Freeman, *J. Magn. Reson.* **44,** 542 (1981).

7. B. Blümich and D. Ziessow, *J. Magn. Reson.* **49,** 151 (1982).

8. A. J. Shaka, J. Keeler, and R. Freeman, *J. Magn. Reson.* **56,** 294 (1984).

9. P. Xu, X-L. Wu, and R. Freeman, *J. Am. Chem. Soc.* **113,** 3596 (1991).

10. P. Xu, X-L. Wu, and R. Freeman, *J. Magn. Reson.* **95,** 132 (1991).

11. M. Woodley and R. Freeman, *J. Magn. Reson. A* **109,** 103 (1994).

12. M. Woodley and R. Freeman, *J. Magn. Reson. A* **111,** 225 (1994).

13. J. J. Titman, A. L. Davis, E. D. Laue, and J. Keeler, *J. Magn. Reson.* **89,** 176 (1990).

14. O. W. Sørensen, M. Rance, and R. R. Ernst, *J. Magn. Reson.* **56,** 527 (1984).

15. A. Abragam, ''The Principles of Nuclear Magnetism,'' p. 497, Clarendon Press, Oxford, England, 1961.

16. A. Kumar, *J. Magn. Reson.* **30,** 227 (1978).

17. G. Bodenhausen, R. Freeman, G. A. Morris, and D. L. Turner, *J. Magn. Reson.* **31,** 75 (1978).

18. L. E. Kay and R. E. D. McClung, *J. Magn. Reson.* **77,** 258 (1988).

19. R. J. Abraham, A. P. Barlow, and A. E. Rowan, *Magn. Reson. Chem.* **27,** 1074 (1989).